Effect of Ultrafine, Fully Vulcanized Acrylate Powdered Rubber on the Mechanical Properties and Crystallization Behavior of Nylon 6

Xuejia Ding, Riwei Xu, Dingsheng Yu, Hong Chen, Run Fan

Key Laboratory for the Preparation and Processing of Novel Polymers, College of Materials Science and Engineering, Beijing University of Chemical Technology, Beijing, 100029, People's Republic of China

Received 30 July 2002; accepted 27 March 2003

ABSTRACT: Nylon 6 (PA6) is a widely used engineering plastic. However, its poor toughness limits its applications. Therefore, toughening PA6 has been a point of interest in the field of PA6 modification. Generally, toughening a plastic with an elastomer reduces the stiffness and heat distortion temperature of the matrix. It has been an important goal of polymer researchers to find a way of toughening PA6 without reductions in its stiffness and heat distortion temperature. In this study, a new kind of material—an ultrafine, fully vulcanized acrylate powdered rubber (UFAPR)—was used to toughen PA6 through melt blending. The influence of UFAPR on the isothermal crystallization kinetics and nonisothermal crystallization behavior of PA was studied with differential scanning calorimetry. The results showed that, with the addition of a little UFAPR, the crystallization rate of PA could be increased, the crystallization temperature could be augmented, and the crystal size distribution of the crystal grain could be narrowed. The changes in the free energy perpendicular to the crystal nucleus were consistent with the results of an Avrami equation according to the theory of Hoffman. The unit surface free energy of the radially developing crystal spherulites decreased with an increasing amount of UFAPR. The results for the mechanical properties, crystalline structure, and crystallization kinetics of PA6/UFAPR composites showed that UFAPR was not only a good toughening agent for PA6 but also an excellent nucleation agent for PA6. © 2003 Wiley Periodicals, Inc. J Appl Polym Sci 90: 3503–3511, 2003

Key words: nylon; nucleation; crystallization

INTRODUCTION

Polyamide (PA) has been developed into many different forms,[1] including PA6 (i.e. nylon 6), PA66, PA11, PA12, PA46, PA610, PA1010, PA612, PA6T, and PA9T.[2,3] PA6T and PA9T have been developed in the last few years, and the output of PA6 and PA66 constitutes more than 80% of the entire yield of PA. Nylon is a crystal plastic, and it possesses an excellent complexation ability over a wide range of temperatures and humidities, but the application of nylon is limited in engineering because of its low impact strength in dry suspensions and at low temperatures. Improving the toughness of PA is currently an area of interest.

Blending a rubber or a thermoplastic elastomer with nylon to improve the material's toughness has been studied the most because the effect is quite distinctive. The first nylon blend grade, PA Zytel St, which was produced by DuPont in 1975, was composed of nylon and a little ultrafine ethylene–propylene–terpolymer rubber modified by the grafting of maleic anhydride. Now, a new patent technology has been applied to the production of an ultratough Zytel resin.[4]

Correspondence to: D. Yu (yuds@mail.buct.edu.cn).

Journal of Applied Polymer Science, Vol. 90, 3503–3511 (2003)

Although the toughness of nylon can be effectively improved by the addition of a traditional rubber or a thermoplastic elastomer, the applications of these materials have been influenced by the loss of strength, the rigidity, and the thermal deformation temperature. Compared with the structure of traditional rubber particles, the structure of ultrafine, fully vulcanized acrylate powdered rubber (UFAPR) is highly crosslinked, and it is obtained during the preparation process.[5] On the one hand, the improvement of the crosslinking degree of the structure can both improve the toughness effect and diminish the modulus loss. On the other hand, the dispersion of UFAPR particles is much smaller than that of traditional rubber particles; therefore, we can achieve enough toughness with only a small amount of UFAPR as long as UFAPR is properly dispersed.

The crystallization process of a polymer plays an important part in the production of composites, and it directly influences the properties of the materials. For a polymer with a low degree of crystallinity (x_c), its melting point, hardness, and rigidity are at a relatively low level. Therefore, crystallization research is very important for the production and use of such products.

The influence of UFAPR on the isothermal and nonisothermal crystallization behavior of PA6 has not

previously been studied. In this study, we have examined the crystallization behavior of PA6/UFAPR and the influence of UFAPR on the dynamic isothermal and nonisothermal crystallization behavior of PA6 with differential scanning calorimetry (DSC) and the crystal structure of PA6/UFAPR with a polarizing microscope (PLM).

EXPERIMENTAL

Raw materials

PA6 (relative viscosity = 2.23) was acquired from Yueyang Petrochemistry Co. (China). UFAPR (grade number vp-301; particle size = 150 nm) was obtained from the Beijing Research Institute of Chemical Industry of China Petroleum and Chemical Corp. (Beijing, China).

Preparation of the samples

Blending of UFAPR and PA6

Dried PA6, UFAPR, and other agents are blended, extruded, and granulated with a twin-screw extruder in a certain ratio.

Polarizing microscopy (PLM)

The temperature of the heading flat was adjusted to 260°C. A little PA6 and the compound were placed between the carrier glass slide and press slide; this was then put into a vacuum oven at a fixed temperature and kept there for 40 min. PLM (20 × 80) was used to observe the crystallization morphology.

Instrumentation

The instrumentation included a ZSK-25WLE reaction twin-screw extruder (Werner and Pfleider Co., Stuttgart, Germany), a DSC-7 differential scanning calorimeter (PerkinElmer Co., Wellesley, MA), an SM-LUX polarizing microscope (Leitz Co., Wetzlar, Germany), an Instron 3211 tensile machine (Instron Co., Massachusetts), an HD-PC heat distortion temperature (HDT) analyzer (Antian Co., Osaka, Japan), a Ceast 6548/000 impact test machine (Ceast Co., Pianezza, Italy), a JSM-35c scanning electron microscope (Hitachi Instruments, Tokyo, Japan), and a TM atomic force microscope (Digital Co., Santa Barbara, CA).

Property testing

Using DSC to test the isothermal crystallization dynamics

The samples were first heated to melting and were kept in a melted state for 5 min. They were then cooled to a certain temperature at a rate of 200°C/min so that the isothermal crystallization curve could be traced. The isothermal temperatures were 194, 195, 196, 197, and 198°C.

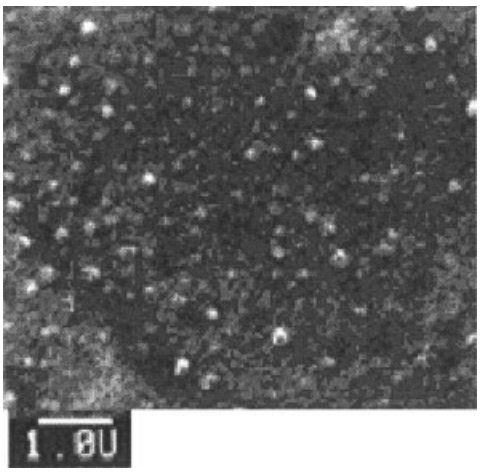

Figure 1 SEM image of UFAPR.

Using DSC to test the nonisothermal crystallization dynamics

For crystallization testing, samples, dropping in temperature at a uniform speed, were kept at 5 min in a melt state and then were cooled to room temperature at a rate of 10°C/min; the temperature, dropping at a uniform speed, was recorded on a crystallization curve.

RESULTS AND DISCUSSION

Characterization of UFAPR

UFAPR consists of white particles. The cohesion between the particles can be hindered by the highly crosslinked structure, and this is beneficial for their dispersion in polymers.

The preparation of UFAPR is as follows. A synthetic acrylate latex is added with a crosslinking agent and high-energy rays to vulcanize the rubber particles in the emulsion. Then, elastic particles can be formed comparable in size to those of rubber particles in the emulsion by the drying of the emulsion.

Figure 1 presents a scanning electron microscopy (SEM) image of UFAPR. The particle of relatively larger size in the image has been formed by the aggregation of several rubber particles, which will be dispersed by the shear force of melting when the aggregate is blended with melted PA6.

Mechanical properties of the PA6/UFAPR composites

Table I shows that the toughness of PA6 increases with the addition of UFAPR. The notch impact

TABLE I
Mechanical Properties of PA6/UFAPR Composites

Composition of PA6/UFAPR	Tensile break strength (MPa)	Elongational at Break (%)	Notch impact strength (J/m)	Bending modulus at 23°C (GPa)	HDT at 1.82 MPa (°C)
100/0	67	55	42	1.8	62.5
100/5	63	101	123	1.7	60
100/10	57.8	70	173	1.58	58.7

strength is increased by 19.3% with the addition of 5 parts of UFAPR, and it is increased by 31.2% with 10 parts of UFAPR.

Generally, the toughness of PA6 is increased by the addition of an elastomer, but when UFAPR is used to toughen PA6, the modulus and HDT of the material are not evidently affected; this indicates that UFAPR is beneficial for nucleation in the crystallization of PA6. This is demonstrated in the following section on crystallization kinetics.

Influence of UFAPR on the isothermal crystallization kinetics of PA6 and its blends

Generally, the isothermal crystallization behavior is tested according to an Avrami equation.[6–8] Because the crystallization enthalpy at a certain temperature changes with time, the related degree of crystallinity at time t [$x(t)$] can be obtained by integration:

$$x(t) = \frac{x_c(t)}{x_c(t_\infty)} = \int_0^t \frac{dH(t)}{dt} \Big/ \int_0^\infty \frac{dH(t)}{dt}\, dt \qquad (1)$$

where $[dH(t)]/dt$ is the rate of the heat flow, $x_c(t)$ is the absolute degree of crystallinity at time t, and $x_c(t_\infty)$ is the crystallinity at the end of the crystallization.

The special form of the equation is

$$x(t) = \frac{x_c(t)}{x_c(t_\infty)} = 1 - \exp[-k(T)t^n] \qquad (2)$$

where n is the Avrami index, which is related to the mode of nuclear formation and growth behavior, and $k(T)$ is the crystallization rate constant at temperature T. Equation (2) can be changed into the following:

$$\log[-\ln[1 - x(t)]] = \log k(T) + n \log t \qquad (3)$$

A beeline can be obtained by $\log\{-\ln[1 - x(t)]\}$ versus $\log t$. The slope is n, and the intercept is $\log k(T)$.

$t_{1/2}$ is the half-crystallization time, and $x(t)$ is 0.5; therefore, the time of crystallization can be calculated:

$$t_{1/2} = [\ln 2/k(T)]^{1/n} \qquad (4)$$

The fastest rate of crystallinity can be obtained if

$$\frac{d^2x(t)}{dt^2} = 0 \qquad (5)$$

Figure 2 presents the DSC isothermal crystallization curves of PA6, and Figure 3 presents the curves of composite materials of PA6/UFAPR. Compared with PA6, the PA6/UFAPR composites have lower induced times and completed times of crystallization, and this shows that the crystallization rate increases with the addition of UFAPR.

Figures 4 and 5 present Avrami-equation-treated isothermal crystallization curves of PA6 and PA6/UFAPR composites, respectively. An excellent linear relationship exists between $\log\{-\ln[1 - x(t)]\}$ and $\log t$ over a wide range of relative degrees of crystallinity, and this means that the isothermal crystallization behavior obeys the Avrami equation. n and $\log k$ can be obtained from the slope and intercept of the beeline, and the results refer to Table II.

Table II shows that that n of PA6 is approximately 2.34, 2.37, 2.39, 2.39, or 2.51 at different crystallization temperatures (T_c's), whereas n of PA6/UFAPR composites is 2.43, 2.44, 2.53, 2.62, or 2.66. According to Morgan's theory,[18] n is an integer that may be 1, 2, 3, or 4, and it depends on the nuclear formation and growth behavior. With respect to three-dimensional growth of a spherulite, n is equal to 3 or 4; for two-dimensional growth of a spherulite, n is equal to 2 or 3; and for one-dimensional growth of a fiber, n is equal to 1 or 2. However, many experiments have shown that heterogeneous nucleation plays the main role in the crystallization process because of the influence of the wall surface and impurities. The process of nuclear formation and the nuclear shape follow the different modes because of the complexity of crystallization. Meanwhile, experimental factors such as the heat history and erroneous determinations at the beginning of crystallization make n nonintegral. All this indicates that n is commonly a decimal fraction and not an integer.[9]

Table II also shows that with an increase in isothermal T_c, for PA6 or PA6/UFAPR composites, t_{max} (time of fastest rate of crystallization) and $t_{1/2}$ increase and k drops with an increase in x_c; this indicates that the

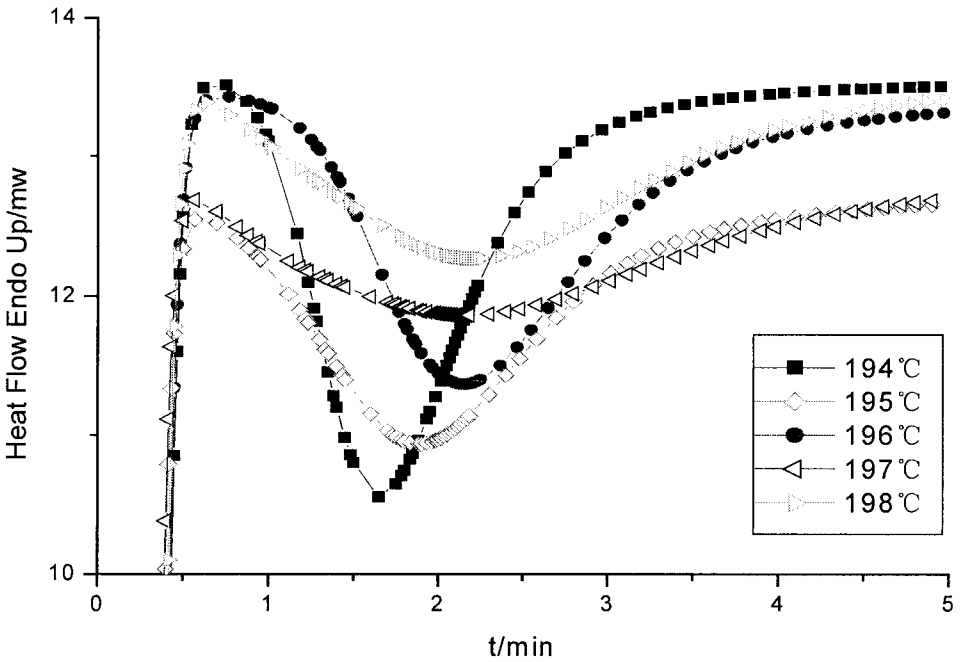

Figure 2 DSC curves of the isothermal crystallization of PA6.

experimental temperature is higher than the temperature of the fastest crystallization rate and that nuclear formation plays the main role in the crystallization process. With a drop in T_c, the crystallization rate quickens because of the increase in nuclear formation, which indicates a drop in $t_{1/2}$. Compared with t_{max} and $t_{1/2}$ of PA6 at the same value of T_c, both t_{max} and $t_{1/2}$ of PA6/UFAPR composites are much lower, and this indicates that UFAPR functions as a nuclear formation agent in different phases during the crystallization process of PA6.

With respect to the numerical values obtained from the Avrami equation, the maximum relative errors of $t_{1/2}$ and t_{max} are about 0.2 and 0.5%, respectively. There is little difference between the value from the experiments and the calculated number, and this shows that the Avrami equation is suitable for explaining the crystallization state.

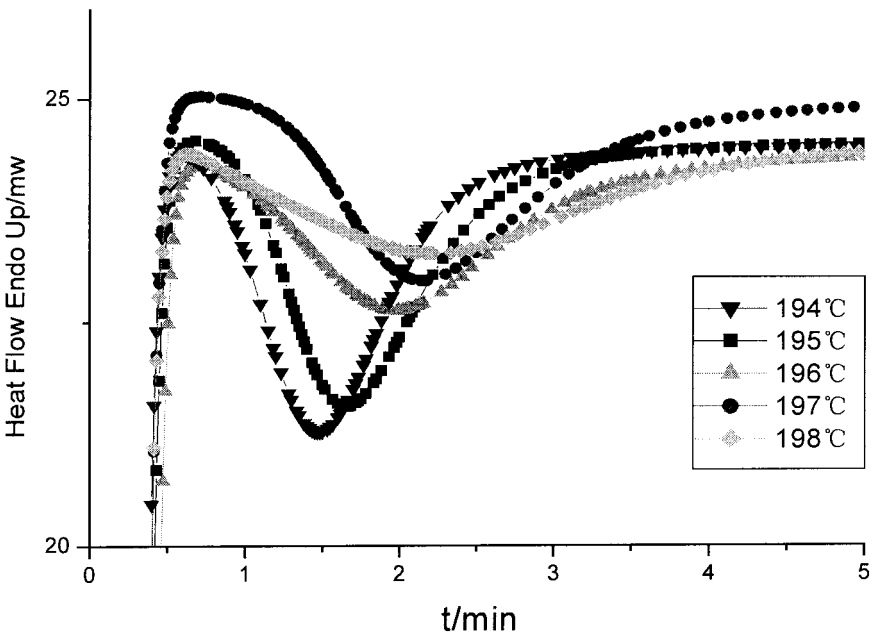

Figure 3 DSC curves of the isothermal crystallization of PA6/UFAPR.

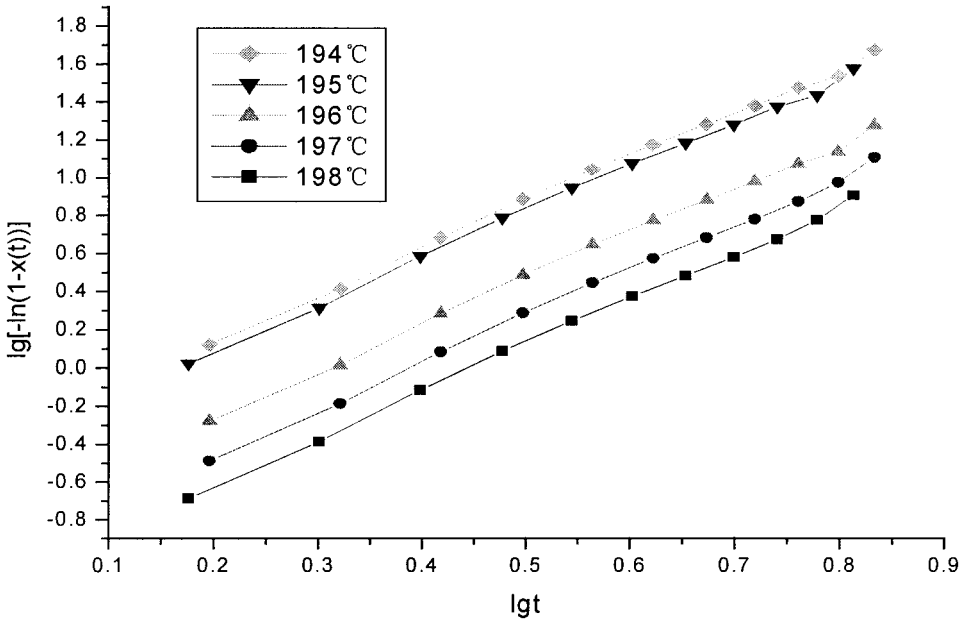

Figure 4 Plots of $\log\{-\ln[1 - x(t)]\}$ versus $\log t$ for the crystallization of PA6.

According to the polymer crystallization theory of Hoffman, the growth rate of the spherulite (G) can be expressed as follows:[10]

$$G = G_0 \exp\left|-\frac{\Delta F}{RT_c}\right| \exp\left|-\frac{k_g T_m^0}{T_c \Delta T}\right| \quad (6)$$

where G_0 is a constant, R is a gas constant, $\Delta T = T_m^0 - T_c$ is the degree of supercooling, and T_m^0 is the balance melting point. When ΔT is low (and T_c is, therefore, high), with an increase in the chain fluidity, the motion of the chain is much easier, and the process of crystallization is controlled by nuclear formation. The crystallization rate of PA6 increases with the addition of UFAPR because of the nuclear formation function of UFAPR. ΔF is the activation energy of a chain moving between the surface of a supercooling liquid and the nuclear formation. ΔF is related to both

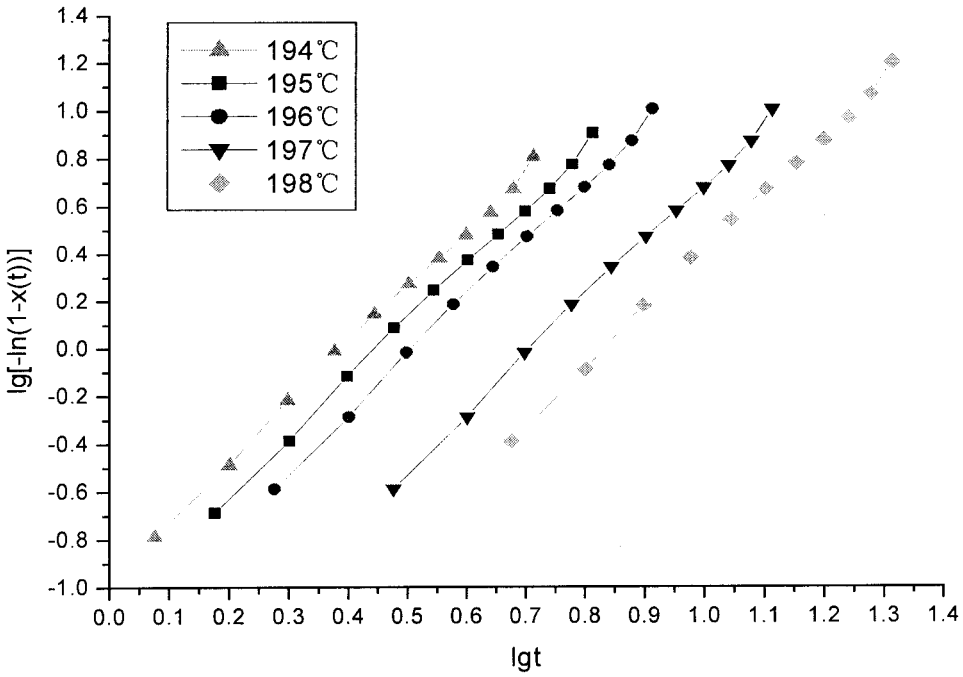

Figure 5 Plots of $\log\{-\ln[1 - x(t)]\}$ versus $\log t$ for the crystallization of PA6/UFAPR.

TABLE II
Parameters of the Isothermal Crystallization Kinetics of PA6 and Its Blends

Sample	T_c (°C)	$-\log k$	$k(s^{-n})$	n	$t_{1/2}$ (s)[a]	t_{max} (s)[b]	$t_{1/2}$ (s)[c]	t_{max} (s)[c]
PA6	194	1.21	0.062	2.51	156.9	148.4	156.5	149.0
	195	1.35	0.0447	2.39	184.9	175.5	184.5	175.3
	196	1.38	0.0417	2.39	194.5	180.7	194.1	181.0
	197	1.40	0.004	2.37	199.9	185.2	199.5	184.8
	198	1.57	0.0269	2.34	240.5	221.7	240.0	220.7
PA6/UFAPR	194	0.95	0.112	2.66	119.0	114.4	119.1	115.0
	195	1.24	0.058	2.62	154.6	148.1	154.1	148.6
	196	1.28	0.052	2.53	167.0	158.2	167.3	158.5
	197	1.32	0.048	2.44	179.2	167.8	179.0	168.1
	198	1.34	0.046	2.43	183.2	171.3	183.5	171.0

[a] Calculated from eq. (5).
[b] Calculated from eq. (4).
[c] Obtained from experimental data.

the molecular structure and temperature and can be obtained from a Williams–Landel–Ferry equation:

$$\Delta F_{WLF} = \frac{C_1 T_c}{C_2 + (T_c - T_g)} \tag{7}$$

$$C_1 = 17.22 \quad \text{kJ/mol}, \quad C_2 = 51.6 \text{ K}$$

$$k_g = \frac{4 b_0 \sigma \sigma_e}{k \Delta H} \tag{8}$$

where b_0 is the thickness of the surface (which is controlled by a nuclear parameter) and σ and σ_e are the interphase free energies of the union area parallel and perpendicular to the chain, respectively. ΔH is the melting enthalpy of crystallization of perfect PA6, and k is the Boltzmann constant.

The Avrami equation shows the isothermal crystallization behavior of the whole polymer sample, whereas Hoffman shows the formation and growth process of each spherulite. The relationship between them can be expressed as follows:[11]

$$G \propto K(T)^{1/n} \tag{9}$$

where G is the nuclear growth rate. $K(T)$ is the crystallization rate constant in the Avrami equation. The ordinary expression of the crystallization rate can be obtained with eq. (6):[12,13]

$$\frac{1}{n} \ln^{K(T)} + \frac{\Delta F_{WLF}}{2.3RT_c} = A_n - \frac{T_m^0}{2.3T_c \Delta T} \tag{10}$$

A beeline can be gained by the construction of $1/n \ln^{K(T)} + (\Delta F_{WLF}/2.3RT_c) - (T_m^0/2.3T_c\Delta T)$ (Fig. 6), and the slope is k_g. σ can be approximately constant because $\sigma_e \gg \sigma$.[14] k_g is obviously proportionate to eq. (8).

In this article, T_m^0 is 501 K, and the glass-transition temperature is 323 K. The k_g values of PA6 and PA6/UFAPR composite materials are 230.9 and 225.4, respectively. This shows that the free energy vertical to the chain decreases and the crystallization rate increases with the addition of UFAPR.

According to the experiment results and the Avrami and Hoffman theory, the crystallization rate can be increased by the addition of UFAPR.

Influence of UFAPR on the nonisothermal cooling crystallization behavior of PA6 and PA6/UFAPR blends

Figure 7 presents the DSC cooling curves of PA6 and PA6/UFAPR composite materials. The peak temperature during the uniform-speed crystallization of PA6 moves to a high temperature and the peak narrows with the addition of UFAPR; this indicates an increase in the crystallization rate.[15]

The uniform-speed-cooling crystallization peak can be analyzed in the following ways:[16] the onset crystallization temperature (T_{onset}), T_c, the beginning slope of the crystallization peak (S_i), the width at the half-height of crystallization peak ($W_{1/2}$), and x_c. Table III shows the parameters of the uniform-speed-cooling crystallization of PA6/UFAPR composite materials.

Table III shows that S_i increases and ΔT decreases ($\Delta T = T_m - T_c$, where T_m is the melting peak temperature of uniform-speed-heating crystallization) by the addition of UFAPR to PA6 materials; this indicates increases in both the rate of nuclear formation and the rate of crystallization of PA6. However, $W_{1/2}$ decreases to some degree, whereas x_c increases a little; this indicates that crystallinity increases.

Influence of UFAPR on the crystallization behavior of PA6

The macromechanical properties of a polymer are closely related to the crystallization behavior and the

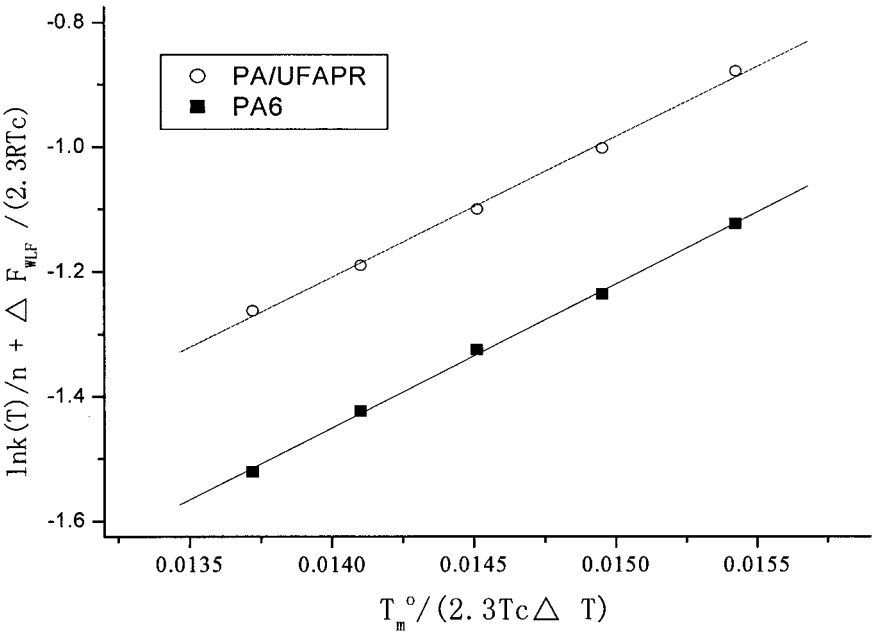

Figure 6 Plots of $(1/n) \times \ln^{K(T)} + (\Delta F_{WLF})/(2.3RT_c)$ versus $T_m^0/(2.3T_c\Delta T)$ for PA6 and PA6/UFAPR.

final crystallite structure. The melting point and stiffness of a polymer will be decreased with an increasing spherulite size, whereas the stiffness and HDT will be increased with a decreasing spherulite size.

The influence of UFAPR on the size of a spherulite can be observed directly with PLM. Figure 8 shows a photograph of the isothermal crystallization of PA6, and Figure 9 shows a photograph of PA6 with UFAPR added (objective lens, 20×; ocular glass, 8×). The practical size can be calculated with the plotting ruler of the object lens, and the data are shown in Table IV.

Figures 8 and 9 show that a spherulite of PA6 has a completed and obviously black cross design. The size of the spherulite is large, and it has an asymmetric distribution. The difference in the radius is large too

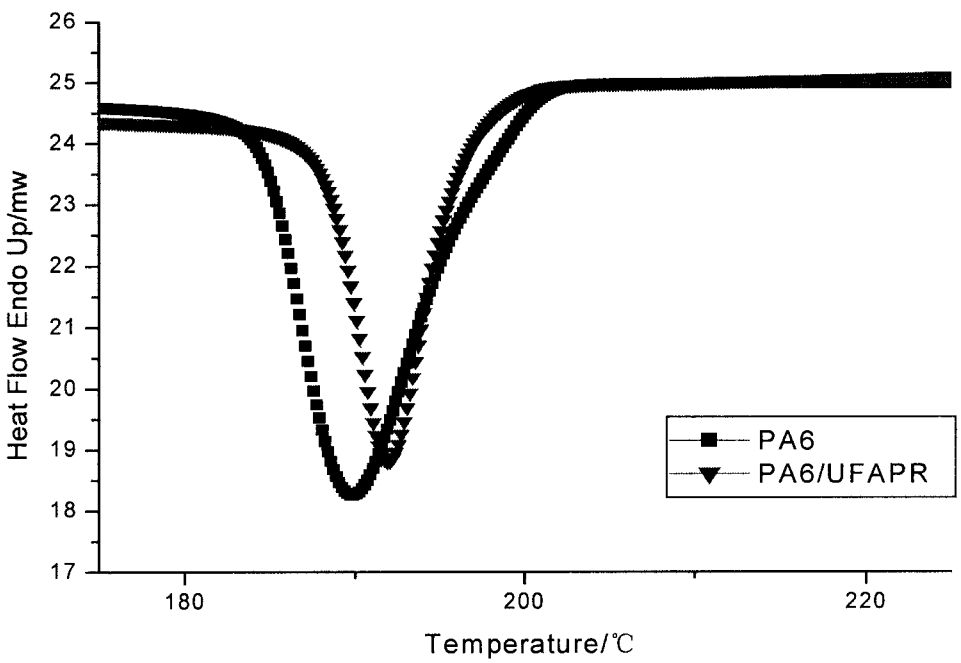

Figure 7 DSC cooling scans (10 K/min) from the melt.

TABLE III
Parameters of the Nonisothermal Crystallization of PA6 and Its Blends

Sample	T_c (°C)	T_{onset}	ΔT (°C)	S_i	$W_{1/2}$	x_c(%)[a]
PA6	189.91	212.45	29.01	6.46	9.43	27.5
Nylon/UFAPR	192.31	206.18	26.79	7.14	7.40	29.5

[a] The heat crystallization of 100% crystalline PA6 is 202.71 J/g.[17]

(16–75 μm), and the average size is 40 μm. When UFAPR is added to PA6, the radius of the spherulite reduces significantly, the number rises, and the distribution becomes more uniform. The black cross design is not as obvious or pure as PA6 because the crystal grains disturb one another, and the integrity of the spherulite drops. In addition, in comparison with PA6, the area of the white part of the PA6/UFAPR composite is much smaller because of the decreased permeation, which indicates the increase of x_c in the composite. This phenomenon is consistent with the results of DSC and reflects the function of UFAPR in PA6. UFAPR acts as a nuclear formation agent and makes the size of the spherulite small and the crystallization rate higher.

Microstructural analysis of the PA6/UFAPR composites

Figure 10 shows that most UFAPR is dispersed uniformly in PA6 and that very few particles exist in the form of aggregates. At the same time, a clathrate structure is formed in the aggregates. The more uniformly rubber particles are dispersed and the lower the number of aggregates is, the more improved the notch impact strength is of a material.

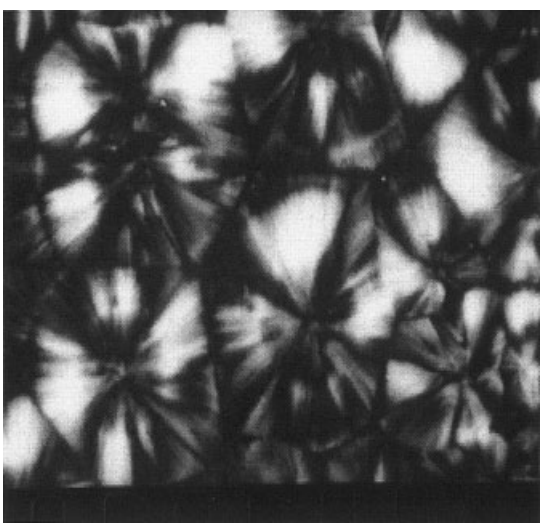

Figure 8 PLM image of pure PA6.

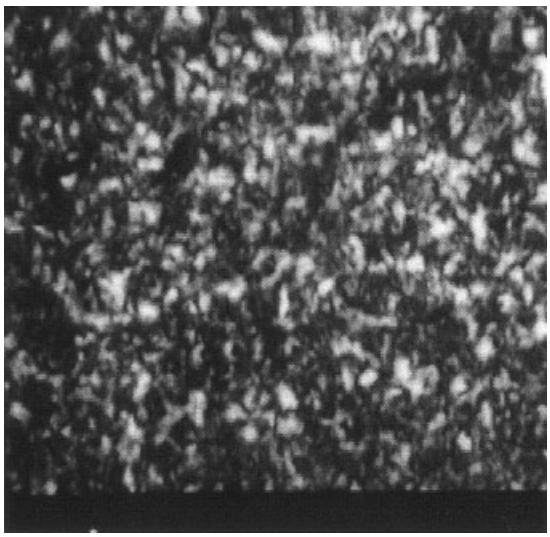

Figure 9 PLM image of a UFAPR/PA6 (100/5) blend.

CONCLUSIONS

A composite with a good balance of stiffness and toughness has been prepared by the modification of PA6 with UFAPR.

The isothermal crystallization behavior of PA6/UFAPR has been studied with DSC. Data from an Avrami equation have shown that t_{max} and $t_{1/2}$ are much lower than those of PA6 at the same value of T_c, and this indicates that the basal nuclear formation mechanism and growth behavior change because UFAPR acts as a nuclear formation function agent in different phases during the crystallization process of PA6. The Hoffman theory shows that the free energy perpendicular to the chain decreases and the crystallization rate of PA6 increases with the addition of UFAPR.

From a study on the influence of UFAPR on the uniform-speed-cooling crystallization behavior of PA6, we have found that $W_{1/2}$ decreases and x_c rises. This means that the distribution of particles is narrowed and that x_c increases, and it indicates that UFAPR acts as a heterogeneous nucleator.

From a study on the influence of UFAPR on the crystallization behavior of PA6 with PLM, we have found that the radius of the spherulite decreases and the number of crystal grains increases with the addition of UFAPR. This indicates that UFAPR acts as a nuclear formation agent, and it makes the spherulite

TABLE IV
Average Spherulite Radius of PA6 and PA6/UFAPR Blends

	PA6	PA6/UFAPR
Average spherulite radius (μm)	40	10

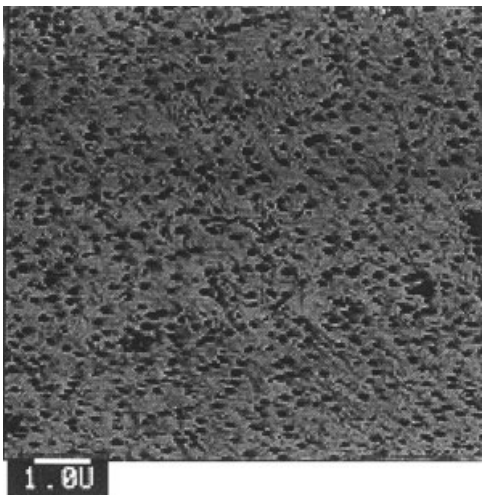

Figure 10 Atomic force microscopy image of a PA6/UFAPR (100/10) composite.

smaller and the crystallization rate higher; these are the most important reasons for increased stiffness of PA6.

A microstructural analysis has shown that most UFAPR is dispersed uniformly in PA6.

The authors thank Jinliang Qiao for his guidance and help.

References

1. Miller, J. R. J Chem Soc 1960, 263, 1311.
2. Hosti-Mietiner, P. M.; Heino, M. T.; Seppala, J V. J Appl Polym Sci 1995, 57, 573.
3. Hu, G. H.; Sun, Y. J.; Lambla, M. J Appl Polym Sci 1996, 61, 1039.
4. Kiss, G. Polym Eng Sci 1987,27, 410.
5. Liu, Y. Q.; Zhang, X.; Wei, G.; et al. Chin J Polym Sci 2002, 20, 93.
6. Avrami, M. J Chem Phys 1939, 7, 1103.
7. Avrami, M. J Chem Phys 1940, 8, 212.
8. Avrami, M. J Chem Phys 1941, 9, 177.
9. Yin, J.; Mo, Z. Modern Macromolecule Physics; Beijing Science: Beijing, China, 2001; p 102.
10. Godovsky, Y. K.; Slonimisky, G. I. J Polym Sci Polym Phys Ed 1974, 12, 1053.
11. Ye, C.; Tang, G.; Liu, J. Acta Polym Sinica 1996, No. 2, 178.
12. Hoffman, J. D.; Weeks, J. J Chem Phys 1962, 37, 1723.
13. Li, D.; Wang, W.; Qi, Z. Acta Polym Sinica 1989, No. 3, 304.
14. Yin, J.; Mo, Z. Modern Macromolecule Physics; Beijing Science: Beijing, China, 2001; p 106.
15. Guan, J.; Sun, C.; Cui, S.; et al. Polym Commun 1981, No. 6, 451.
16. Gupta, A. K.; Gupta, V. B. J Appl Polym Sci 1982, 27, 4669.
17. Chao, L.; Chang, E. J Appl Polym Sci 1981, 26, 603.
18. Morgan, L. B. Phil Trans Royal Soc (London) 1954, A247, 13.